World Academy of Science, Engineering and Technology
International Journal of Energy and Power Engineering
Vol:9, No:4, 2015

Thermodynamic Cycle Analysis for Overall Efficiency Improvement and Temperature Reduction in Gas Turbines

Jeni A. Popescu, Ionut Porumbel, Valeriu A. Vilag, Cleopatra F. Cuciumita

***Abstract*—**The paper presents a thermodynamic cycle analysis for three turboshaft engines. The first cycle is a Brayton cycle, describing the evolution of a classical turboshaft, based on the Klimov TV2 engine. The other four cycles aim at approaching an Ericsson cycle, by replacing the Brayton cycle adiabatic expansion in the turbine by quasi-isothermal expansion. The maximum quasi-Ericsson cycles temperature is set to a lower value than the maximum Brayton cycle temperature, equal to the Brayton cycle power turbine inlet temperature, in order to decrease the engine NO_x emissions. Also, the power/expansion ratio distribution over the stages of the gas generator turbine is maintained the same. In two of the considered quasi-Ericsson cycles, the efficiencies of the gas generator turbine, as well as the power/expansion ratio distribution over the stages of the gas generator turbine are maintained the same as for the reference case, while for the other two cases, the efficiencies are increased in order to obtain the same shaft power as in the reference case. For the two cases respecting the first condition, both the shaft power and the thermodynamic efficiency of the engine decrease, while for the other two, the power and efficiency are maintained, as a result of assuming new, more efficient gas generator turbines.

***Keywords*—**Combustion, Ericsson, thermodynamic analysis, turbine.

I. Introduction

THE idea of a of a gas turbine engine employing isothermal turbine expansion was first advanced by the Swedish inventor John Ericsson in 1853 [1], as part of a thermodynamic cycle that bears his name, the Ericsson cycle engine, and which is formed by isothermal compression and expansion, and isobaric heat addition and rejection.

Serious research efforts have been carried out over the years on the isothermal compression with reasonable success, in particular using water injection. Practical solutions for isothermal expansion are, on the contrary, not available today.

Turbine combustion is a recent concept, and the amount of work in the field is presently quite limited. An extensive review of recent work in the field [2] is focusing on four related areas: (i) thermodynamic cycle analysis, (ii) reacting mixing layers in accelerating flows, (iii) flame holding in high speed flows and (iv) compact combustors.

Thermodynamic cycle analysis has been carried out for both continuous combustion [3], and for inter-stage combustion [4], using component efficiencies based on typical, real life, values, and demonstrating performance gains related to lower fuel consumption, higher specific thrust, and enhanced operational speed and compressor pressure ratios for both turbojet and turbofan engines. The results are clearly showing benefits of the technology. Unlike this situation, the three last research areas are facing known difficult problems and only recently developed investigation methods promise to be able to handle them. It explains the current lack of understanding when they are present simultaneously and quantifies the challenge of performing stable combustion in the turbine.

Considering each area separately, we start with combustion in accelerating flows. It has been mainly studied for low Mach number reacting mixing and boundary layers, mostly for laminar [5]-[8], but also some turbulent [9], [10] flows. High speed reacting layers, as is the case of the problem proposed here, are scarcer, but some results on high speed flow combustion have been published [11]-[16]. Theoretical, similarity studies of laminar, two-dimensional, reacting, accelerating mixing layers [17] have shown a decrease of the peak temperature along the mixing layer, with beneficial effects upon the formation of NOx. The work has been extended to non-similar cases using one-step finite rate chemistry in laminar [18] and turbulent [19] flows using the boundary layer approximation. Three-dimensional, full Navier-Stokes numerical simulation studies of accelerating, reacting flows are very limited at this moment, but some simple geometry attempts have been reported [20], [21], also including some limited experimental validation [22]. The key finding of these studies is that fully developed turbulence cannot be assumed in the turbine channels, so RANS based numerical simulations are not suited for the problem, requiring more advanced LES numerical simulations. Numerical simulations [23], [24] on premixed and partially premixed reacting, accelerating and curved flow, aimed at assessing the effect of the centrifugal forces in the rotating part of the turbine, but had limited success due to the two-dimensional approach. Experimental studies [25]-[28] of ignition, stabilization and combustion of liquid fuelled flames in high centrifugal acceleration flows have been carried out in recent years at the Air Force Research Laboratories, in the United States.

J. A. Popescu, V. A. Vilag, and C. F. Cuciumita are with the Romanian Research and Development Institute for Gas Turbines COMOTI, Department of Aviation and Industrial Turbines. Gas Turbine Package, Bucharest, 061126, Romania (phone: +40-21-434-01-98; fax: +40-21-434-02-41; e-mail: jeni.popescu@comoti.ro, valeriu.vilag@comoti.ro, cleopatra.cuciumita@comoti.ro).

I. Porumbel is with the Romanian Research and Development Institute for Gas Turbines COMOTI, Department of Combustion Chambers and Unconventional Energies, Bucharest, 061126, Romania (e-mail: ionut.porumbel@comoti.ro).

For area (iii), the flame stabilization mechanism in high speed flow has been investigated in the light of hypersonic vehicles, for example Scramjet applications. Important contributions originated from the Air Force Research Laboratories featuring liquid injection of fuel into supersonic cross-flow has been studied [29], [30]. Another set of studies [31], [32] aimed at determining the fuel distribution resulting from low angle fuel injection along the solid wall in supersonic, non-reactive flows. Reactive flow experimental measurements were also reported, and the flame stabilization role of a cavity placed on the solid wall has been analyzed for various injector designs [33], [34]. Combustion of Kerosene injected in supersonic flows and stabilized using a Hydrogen pilot flame and various cavity patterns, as well as the effect of aeration in conjunction with the cavity geometry and the impact of the flow conditions (temperature and pressure) on the ignition delay were experimentally studied [35], [36], indicating combustion efficiency up to 92 %.

The flame stabilization mechanism in high speed flows, that plays a critical role in turbine combustion, has mainly been studied from the standpoint of supersonic combustion for Scramjets and Ramjets, and differs for the case considered here, even if benefits from the insight gained in those studies are relevant. In particular, the presence of a recirculation region in the flow enables the fuel and the air mixing and burning. Coherent structures, detaching from the recirculation region and containing unburned mixture and burning pockets are carried downstream, further contributing to the complete combustion of the injected fuel [37]. The recirculation region can be created by placing in the flow a cavity [38], or a step [39], creating a sudden flow expansion, and by injecting fuel and, possibly, air, in that reversed flow region. These solutions, generically termed Compact Combustors [37], provide low pressure drop flame stabilization and are already tested for non-accelerating low speed flow.

The Trapped-Vortex Combustor [39] (TVC) was first proposed by the Air Force Research Laboratory and General Electric Aircraft Engines, in the United States, during the last decade. In this approach, the flame is stabilized by means of a vortex trapped in a cavity created on the burner walls, acting as a pilot flame by recirculating the hot burned gas in the cavity, as fuel and air are continuously injected in the cavity. Preliminary experimental [40] and numerical [41], [42] studies have shown that the TVC can not only provide stable combustion, but can also decrease the NOx emissions. Experimental and numerical studies of cavity stabilized, gas fuelled flames in a flow passage resembling turbine stator blades have been reported by [37]. Variants or improvements of the TVC include the Ultra Compact Combustor [30] (UCC) and the Cavity Inside Cavity [43] (CVC). The UCC and CVC locate the cavity circumferentially with the idea of allowing for most of the combustion to take place around the turbine shroud. It strongly reduces the axial dimension of the combustion zone [37]. Low pressure experimental measurements on UCC were carried out [44] with promising results regarding combustion efficiency, combustor compactness, flame stability, especially for lean mixtures, and heat release ratio. It is, however, unclear if the concept performs at higher pressure and how it reacts to higher temperature vitiated air.

Alternative concepts are the Inter Turbine Burning (ITB) and In Situ Combustor (ITC) [45]. For the first one, supplementary combustion occurs between the high and the low pressure turbines, acting as a reheating stage in a rough approximation of an Ericsson cycle. The In Situ Combustor [46] is the existing concept closest to the needs of the proposed project. Developed by Siemens Westinghouse Power Corporation, the concept proposes fuel injection through the airfoils in order to reheat the expansion cooled gas to increase the cycle efficiency towards the ideal Ericsson cycle efficiency and power output, and to reduce the NOx emissions [37]. However, the ability of achieving stable and complete combustion in the turbine flow channels between the blades and vanes has not yet been demonstrated. In particular, the very short residence time is often lower than the auto-ignition delay, and stabilization requires an additional means, such as a cavity feeding with burn gases.

The work presented here focuses on the idea of turbine combustors, that will maintain the expansion process as close as possible to isothermal. This turbine, or secondary, combustion, as opposed to the main combustion occurring in the gas turbine engine main combustion chamber, takes over part of the main combustion such that the overall engine power remains as much unchanged as possible, while providing a smaller cycle maximum temperature and a smaller temperature variation throughout the combustion process.

The main advantage of the approach presented here is NO_x and pollutant emission reduction and promising to be a major contributor to the European Commission's Flightpath 2050 target of 90% NO_x reduction per passenger and per kilometre [47].

Decreasing the combustor temperature will also impact on the need for costly combustor materials and thermal barrier coatings on the combustor liner, enabling a more resource efficient manufacturing.

Due to the distributed fuel injection and combustion, both in the main combustor and in the turbine combustor, the amount of fuel to be burned at each location is smaller, thereby allowing a more complete and efficient combustion, decreasing the amount of Unburned Hydrocarbons (UHC) and also the emission of solid particles (e.g. soot), creating the premises for a greener aircraft engine.

In practical applications, however, a fully isothermal turbine cannot be achieved, since it will require infinitesimal heat addition to compensate the work produced in the turbine rotor. Instead, the thermodynamic analysis proposed here focuses on a secondary combustion process that occurs between the turbine stages of a two-staged gas generator turbine of a two spool turboshaft, in a first approximation of an isothermal expansion cycle.

The objectives of the work presented here are to evaluate the effect of the secondary combustion process occurring between the two stages of the gas generator turbine on the thermodynamic performances of the engine, and to determine

the turbines parameters modifications required to increase or maintain the gas turbine engine thermodynamic performances above the reference one (without secondary combustion), while decreasing the maximum thermodynamic cycle temperature.

To achieve these objectives, the maximum temperature of the main combustion process is decreased to the value corresponding to the temperature value at the inlet of reference engine power turbine, while allowing for minimal engine constructive modifications. For this, the engine inlet, compressor, power turbine, and nozzle will remain unchanged in this analysis.

II. Problem Formulation

A. Operating Conditions

The goal of the study is to analyze, by comparison to a reference classical two spool, two plus one turbine stages turboshaft of similar configuration, the trends in the fuel consumption and the efficiency of such a combustion turbine. The studied combustion turbine operates under the assumptions that the two compared engines operate under the same thermodynamic conditions both at the compressor outlet and at the power turbine inlet, and that, in the combustor turbine case, the temperature is the same at the main combustor outlet and at the power turbine inlet.

To satisfy these conditions, the fuel mass flow rate injected into the main combustor is decreased in the combustor turbine case compared to the reference turboshaft, and an additional amount of heat is introduced between the gas generator turbine stages.

It is also assumed that the gas generator turbine power balances the compressor power consumption. To further enable a meaningful comparison, the environmental operating conditions are maintained identical (standard atmospheric conditions [48]) both for the reference gas turbine engine and for the combustor turbine engine. The diagrams of the two types of engines are provided in Figs. 1 and 2.

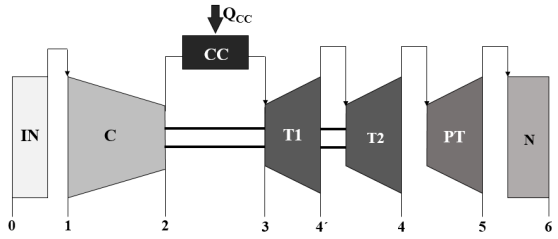

Fig. 1 Diagram of the reference turboshaft configuration

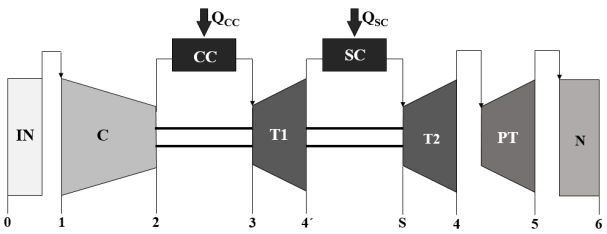

Fig. 2 Diagram of the modified turboshaft configuration

In Fig. 1 and 2, "IN" represents the engine inlet, "C" is the compressor, "T1" and "T2" are the two stages of the gas generator turbine, "PT" stands for the power turbine, and "N" designates the engine exhaust nozzle, while "CC" and "SC" represent the main and secondary combustions

B. Initial Conditions

The turboshaft inlet conditions correspond to the standard atmospheric conditions at sea level [48]:

$$T_0 = 288\ K \tag{1}$$

$$p_0 = 101{,}325\ Pa \tag{2}$$

The compression ratio was set to [49]:

$$\pi_C = 7.2. \tag{3}$$

Gas constant for air [48]:

$$R = 287.3 J/kg \cdot K. \tag{4}$$

The efficiencies and loss coefficients of the engine components used in here and presented below, were determined based on [49], as follows:

Inlet pressure loss coefficient:

$$\sigma_{IN} = 0.99 \tag{5}$$

Compressor efficiency:

$$\eta_C = 0.82 \tag{6}$$

Main combustion efficiency:

$$\eta_{CC} = 0.97 \tag{7}$$

Main combustor pressure loss coefficient:

$$\sigma_{CC} = 0.96 \tag{8}$$

Gas generator turbines efficiencies:

$$\eta_T = \eta_{T1} = \eta_{T2} = 0.83 \tag{9}$$

Secondary combustion efficiency:

$$\eta_S = 0.97 \tag{10}$$

Secondary combustion pressure loss coefficient:

$$\sigma_S = 0.96 \tag{11}$$

Mechanical efficiency of the compressor - gas generator turbine transmission:

$$\eta_m = 0.995 \quad (12)$$

Power turbine efficiency:

$$\eta_{PT} = 0.84 \quad (13)$$

Nozzle velocity loss coefficient:

$$\varphi_N = 0.995 \quad (14)$$

To simplify the calculations and to allow a clear evaluation of the effect of adding heat between the gas generator turbine stages, unconfounded by the effects induced by the chemical transformations occurring in the working fluid due to combustion, the working fluid for all the thermodynamic evolutions presented here is air, both the main combustion and the turbine combustion being modelled by simple heat addition to the system.

C. The Studied Cases

The reference case describes the thermodynamic cycle of a known turboshaft engine (Klimov TV2-117A) [49], its configuration being presented in Fig. 1.

Cases 1 and 3

While maintaining the main combustion temperature equal to the temperature value at the inlet of reference engine power turbine, heat is added between the two stages of the unmodified gas generator turbine. The analysis aims at determining the required amount of secondary heat to be added such that the power generated by the gas generator turbine to be just sufficient to drive the engine compressor

Cases 2 and 4

As before, the main combustion temperature is maintained equal to the temperature value at the inlet of reference engine power turbine, and heat is added between the two stages of the gas generator turbine. In these cases, though, the existence of a new, superior efficiency gas generator turbine is assumed, such that the turboshaft engine power, respectively the expansion ratio, remains the same as in the reference engine case. To simplify the calculations, the two stages of the gas generator are assumed of equal efficiency. The analysis aims at determining the required efficiency of the new gas generator turbine, such that all thermodynamic parameters are maintained unchanged at the power turbine inlet. The amount of secondary heat to be added remains just sufficient to allow the power generated by the gas generator turbine to drive the engine compressor.

D. Thermodynamic Evolutions and Governing Equations

The method for determining the ideal and the real total thermodynamic parameters on all the main sections of the reference and modified gas turbine engine (identified in Figs. 1 and 2) is presented in the following, according to [50].

In general, the problem of determining the parameters of a thermodynamic evolution reduces to determining the values of two of the total parameters: pressure (p), temperature (T), enthalpy (h), and entropy (s), while the other two are known. For some of these cases, polynomial curve fitting functions relating temperature and enthalpy, respectively temperature and entropy at the atmospheric pressure exist in the literature [47] and will be used in the following.

Case 0:

Section 0 corresponds to a position upstream of the engine inlet.

The standard atmospheric conditions are known and h_0 and s_0 are determined using the polynomial curve fitting functions.

Admission. Section 1 corresponds to a position downstream of the engine inlet. The engine inlet is assumed cylindrical, hence only losses in the total pressure occur in the real admission:

$$T_1 = T_0, \quad (15)$$

$$p_1 = p_0 \cdot \sigma_{IN}. \quad (16)$$

The entropy at a given temperature and pressure, can be determined from the entropy at the same temperature and atmospheric pressure by using [48]:

$$s_1 = s_{10} \cdot R \cdot \ln \frac{p_0}{p_1}. \quad (17)$$

where the entropy at the same temperature and atmospheric pressure is given by the corresponding polynomial curve fitting function mentioned earlier. In this case, the reference state is the known State 0.

The enthalpy h_1 is determined using the corresponding polynomial curve fitting function. The ideal State 1 is identical to State 0.

Compression. Section 2 corresponds to the compressor outlet, also coinciding with the combustor inlet. The air compression is assumed adiabatic. The ideal compression, State 2id, is reached from state 1 through an isentropic adiabatic compression:

$$s_{2id} = s_1. \quad (18)$$

The pressure can be determined knowing the compressor pressure ratio, given by (3), and is the same in the states 2id and 2:

$$p_2 = p_{2id} = p_1 \cdot \pi_C. \quad (19)$$

The temperature, and then the enthalpy can be determined using the polynomial curve fitting functions.

State 2, the real compression is reached, from State 1, through a non-isentropic adiabatic compression. For State 2, the path 1 - 2 is still adiabatic, but not isentropic anymore. Instead of the ideal work, defined as [50]

$$w_{Cid} = h_{2id} - h_1, \quad (20)$$

the real compressor work will be used to bring the air in State 2id [50]:

$$w_C = h_2 - h_1 = \frac{w_{Cid}}{\eta_C}. \quad (21)$$

By combining (20) and (21), the State 2 enthalpy is

$$h_2 = h_1 + \frac{h_{2id} - h_1}{\eta_C}. \quad (22)$$

The temperature T_2 is determined using the corresponding polynomial curve fitting function. The entropy at State 2 can be determined by using first the corresponding polynomial curve fitting function to determine the entropy at temperature T_2 and atmospheric pressure, and then (17).

Combustion. Section 3 corresponds to the main combustor outlet, also coinciding with the first stage gas generator turbine inlet. Combustion is modelled as heat addition at constant pressure in the ideal case, and with a known pressure loss in the real case:

$$p_{3id} = p_{2id}, \quad (23)$$

$$p_3 = p_3 \cdot \sigma_{CC}. \quad (24)$$

For the reference engine in Case 0, the amount of fuel burned in the main combustor is known [49]:

$$\dot{M}_{f0} = 0.1145 kg/s. \quad (25)$$

The specific heat added to the thermodynamic cycle in the main combustor can be, then, determined as [50]

$$Q_{CC} = \frac{\dot{M}_{f0} \cdot h_f \cdot \eta_{CC}}{\dot{M}_{f0} + \dot{M}_a}, \quad (26)$$

where h_f is the specific heat of combustion and the air mass flow rate through the engine is

$$\dot{M}_a = 7.3162 kg/s. \quad (27)$$

In the ideal case, the combustion efficiency in the main combustor is assumed unity, therefore

$$Q_{CCid} = \frac{\dot{M}_{f0} \cdot h_f}{\dot{M}_{f0} + \dot{M}_a}, \quad (28)$$

$$Q_{CC} = Q_{CCid} \cdot \eta_{CC}. \quad (29)$$

Since no work is either produced, or consumed in the main combustor, according to the first principle of thermodynamics [48],

$$h_{3id} = h_{2id} + Q_{CC} \quad (30)$$

and

$$h_3 = h_2 + Q_{CC}. \quad (31)$$

Knowing h_{3id} and h_3, the temperatures T_{3id} and T_3, and then the ideal and real entropies at atmospheric pressure can be determined using the polynomial curve fitting functions, and the entropies s_{3id} and s_3 are given by (17).

Expansion in the first stage of the gas generator turbine. Section 4' corresponds to the gas generator turbine first stage outlet, also coinciding with the first stage gas generator turbine inlet. The expansion is assumed adiabatic. State 4'id, the ideal expansion, is reached from State 3 through an isentropic adiabatic expansion, while State 4', the real expansion, is reached through a non-isentropic adiabatic expansion.

The turbine work required to drive the engine compressor must be provided by the two stages of the gas generator turbine and is, ideally,

$$w_{Tid} = \frac{w_C}{\eta_m}. \quad (32)$$

The gas generator turbine work is divided between the two gas generator turbine stages such that the first stage produces 40% of the total work (w_{T1}), and the second stage produces the remaining 60% of the total work (w_{T2}):

$$w_{T1id} = 0.4 \cdot w_{Tid}, \quad (33)$$

$$w_{T2id} = 0.6 \cdot w_{Tid}. \quad (34)$$

The ideal enthalpy can be expressed as

$$h_{4'id} = h_3 - w_{T1id}. \quad (35)$$

The temperature $T_{4'id}$ and the entropy at the same temperature and atmospheric pressure can be found using the polynomial curve fitting functions. Since path 3 - 4'id is isentropic,

$$s_{4'id} = s_3, \quad (36)$$

the pressure $p_{4'id}$ can, then, be determined using (17).

The real expansion occurs between the same pressures as the ideal expansion, hence

$$p_{4'} = p_{4'id}. \quad (37)$$

The real cycle enthalpy can be determined based on the real work produced by the first stage of the gas generator turbine:

$$h_{4'} = h_3 - w_{T1id} \cdot \eta_{T1}. \quad (38)$$

The temperature $T_{4'}$ and the entropy $s_{4'}$ at the known temperature and pressure can be found using the

corresponding polynomial curve fitting functions.

Expansion in the second stage of the gas generator turbine. Section 4 corresponds to the gas generator turbine second stage outlet, also coinciding with the power turbine inlet. For Case 0, the same procedure for determining the thermodynamic parameters in State 4 applies, as for State 4':

$$s_{4id} = s_{4'}, \tag{39}$$

$$h_{4id} = h_{4'} - w_{T2id}. \tag{40}$$

Temperature T_{4id} and the entropy at the same temperature and atmospheric pressure are found using the polynomial curve fitting functions, and pressure p_{4id} is determined using (17).

For the real State 4:

$$p_4 = p_{4id}, \tag{41}$$

$$h_4 = h_{4'} - w_{T2id} \cdot \eta_{T2}. \tag{42}$$

The temperature T_4 and the entropy s_4 at the known temperature and pressure can be found using the corresponding polynomial curve fitting functions.

Expansion in the power turbine. Section 5 assumes the pressure slightly higher than the atmospheric pressure:

$$p_5 = p_{5id} = \frac{p_0}{\sigma_N} \tag{43}$$

$$\sigma_N = 0.99 \tag{44}$$

Similarly to the other turbines, the ideal parameters are calculating assuming an isentropic process.

The ideal entropy at atmospheric temperature is determined using (17), then the temperature T_{5id} and the enthalpy h_{5id} are obtained using the polynomial curve fitting functions.

The ideal power turbine work is

$$w_{5id} = h_4 - h_{5id}, \tag{45}$$

while the real work is

$$w_5 = w_{5id} \cdot \eta_{PT}. \tag{46}$$

The enthalpy h_5, then the temperature T_5 and entropy s_5 are calculated similarly to the previous sections.

Expansion in the exhaust nozzle. Section 6 corresponds to the exit section of the gas turbine engine. State 6id, the ideal expansion, is reached from State 5 through an isentropic expansion, while State 6, the real expansion, is reached through a non-isentropic expansion, with assumed velocity losses.

Since path 5 - 6id is isentropic and

$$p_{6id} = p_0, \tag{47}$$

The ideal entropy at atmospheric pressure can be determined by using (17), and then the temperature T_{6id} and the enthalpy h_{6id} with the help of the polynomial curve fitting functions.

Calculating the ideal velocity

$$c_{6id} = \sqrt{2000 \cdot (h_5 - h_{6id})}, \tag{48}$$

and assuming the velocity losses

$$c_6 = c_{6id} \cdot \varphi_N, \tag{49}$$

The real enthalpy is determined using (48), then the temperature T_6 and the entropy, determined using the polynomial curve fitting functions and (17), will completely define State 6.

The cycle is closed by a fictitious isobar that connects State 6 and State 0.

Cases 1 - 4:

For the turbine combustion engines in the other four cases, the maximum cycle temperature is fixed at the same value as the reference power turbine inlet temperature (to be determined later):

$$T_3 = T_{4ref}. \tag{50}$$

The enthalpy h_3 is determined using the corresponding polynomial curve fitting function, and the heat added to the system in the real case is

$$Q_{CC1} = Q_{CC2} = h_3 - h_2. \tag{51}$$

The amount of fuel required to release through combustion this heat is

$$\dot{M}_{f1} = \dot{M}_{f2} = \dot{M}_a \cdot \frac{Q_{CC1}}{\eta_{CC} \cdot h_f - Q_{CC1}} = \dot{M}_a \cdot \frac{Q_{CC2}}{\eta_{CC} \cdot h_f - Q_{CC2}}. \tag{52}$$

In the ideal case, the same enthalpy raise requires less fuel:

$$\dot{M}_{f1} = \dot{M}_{f2} = \dot{M}_a \cdot \frac{Q_{CC1}}{h_f - Q_{CC1}} = \dot{M}_a \cdot \frac{Q_{CC2}}{h_f - Q_{CC2}}. \tag{53}$$

Knowing T_3, the ideal and real entropies at atmospheric pressure can be determined using the polynomial curve fitting functions, and the entropies s_{3id} and s_3 are given by (17).

The expansion in the gas generator turbine can be further subdivided into an expansion in the first stage of the gas generator turbine, Section 4', and an expansion in the second stage of the gas generator turbine, Section 4.

Case 1

In Case 1, the temperature at the gas generator turbine outlet is fixed at the same value as the reference T_4 and the efficiencies of the two stages of the gas generator turbine are kept the same as in Case 0.

Expansion in the first stage of the gas generator turbine. Section 4' corresponds to the gas generator turbine first stage outlet, also coinciding with the turbine combustor inlet. As for the reference case, the expansion is assumed adiabatic, isentropic for the ideal evolution, and non-isentropic for the real one.

The turbine work required to drive the engine compressor is given by (32) and the ideal gas generator turbine work is divided between the two gas generator turbine stages, similar to Case 0, such that the first stage produces 40% of the total work (w_{T1}), and the second stage produces the remaining 60% of the total work (w_{T2}), as in (33) and (34). The ideal enthalpy can be given by (35). The thermodynamic parameters in Section 4' are determined with the same method as for Case 0, using the relations given by (35)–(38).

Secondary combustion between the two stages of the gas generator turbine. Section S corresponds to the turbine combustor outlet, also coinciding with the gas generator turbine second stage inlet.

As for the main combustion, the process is modelled as heat addition at constant pressure in the ideal case, and with a known combustion pressure loss in the real case:

$$p_{Sid} = p_{4'}, \tag{54}$$

$$p_S = p_{Sid} \cdot \sigma_{SC}. \tag{55}$$

The amount of heat added through secondary combustion, Q_{SC}, is chosen such that the work produced by the gas generator turbine just balances the work consumed by the compressor, and is determined iteratively, to satisfy this condition.

Since no work is either produced, or consumed in the turbine combustor,

$$h_S = h_{4'} + Q_{SC}. \tag{56}$$

Knowing h_S, the temperature T_S, and then the ideal and real entropies at atmospheric pressure can be determined using the polynomial curve fitting functions. Entropy s_S is given by (17).

In the ideal case, the heat produced through combustion using the same amount of fuel is larger:

$$Q_{SCid} = \frac{Q_{SC}}{\eta_{SC}}. \tag{57}$$

Hence, the ideal enthalpy is

$$h_{Sid} = h_{4'} + Q_{SCid} \tag{58}$$

The temperature and the entropy for the ideal State Sid are determined similarly to the real case.

Expansion in the second stage of the gas generator turbine. Section 4 corresponds to the gas generator turbine second stage outlet, also coinciding with the power turbine inlet.

As mentioned before, the temperature T_4 at the gas generator turbine outlet is known, fixed at the same value as in Case 0.

Starting from the required turbine work given by (34) and assuming an adiabatic, isentropic ideal evolution, and a non-isentropic real one, the parameters are calculated similarly to Case 0.

Case 2

Case 2 aims to maintain the conditions in the reference Section 4, the temperature and the pressure at the gas generator turbine outlet, are fixed at the same values as in Case 0. The particularity of this case is that the efficiencies of the two stages of the gas generator turbine are determined in order to balance the gas generator work.

While Section 3 is identical to the same section in Case 1, therefore completely determined, a series of parameters in Section 4´ can be calculated. The ideal turbine work respecting (33), the enthalpy $h_{4'id}$, the temperature $T_{4'id}$ and the entropy at atmospheric temperature can be determined. The entropy $s_{4'id}$ is known based on the assumption that the ideal process is isentropic, therefore the known parameters allow for calculating the pressure using (17). The real parameters are then easily calculated similarly to previous cases.

The parameters and the turbine work in Section 4 are set at equal values as in Case 0, allowing for the calculation of Section S, with the same added heat value as in Case 1. The gas generator work balancing is achieved for new turbines with the theoretical efficiency of 0.943.

Case 3

In Case 3, the calculation method is similar to that used in Case 1, fixing the temperature at the gas generator turbine outlet is at the same value as the reference T_4 and maintaining the efficiencies of the two stages of the gas generator turbine as in Case 0. The difference occurs from maintaining the expansion ratio distribution on the two stages of the gas generator, as in Case 0, while balancing the gas generator work. The heat addition in Section S is determined iteratively in order to satisfy this condition.

Case 4

Similarly to Case 2, Case 4 aims to maintain the conditions in the reference Section 4. Section 3 is completely determined, as in the previous cases, as well as Section 4, as in Case 2. The condition of balancing the gas generator work is respected by determining the increased efficiencies of the two stages of the gas generator turbine. The gas generator work balancing is achieved for new turbines with the theoretical efficiency of 0.933.

Cases 1 and 2 are presented comparatively, along with reference Case 0, in the results section of the paper, in Fig. 3.

Similarly, Cases 3 and 4 are presented in Fig. 4.

III. Results and Discussion

The numerical results of the previously presented algorithm applied for the five considered turboshaft cycles are presented in Tables I–V, and the *s*-*T* diagrams of the thermodynamic

cycles are presented in Figs. 3–5.

It can be noted that even if the maximum temperature in the main combustor for the combustion turbine cases decreases significantly, by 235 K, the decrease in the maximum cycle temperature is smaller, in the 73–93 K range, due to the secondary combustion. This effect will need to be considered when selecting the materials and technologies for the manufacturing of the two gas generator turbines, since the thermal load is larger for the second stage than for the first stage in the combustion turbine cases. It is also important to note that the exhaust enthalpy for Case 1 is larger than for Cases 0 and 2, indicating a larger energy loss in the engine exhaust. A similar difference can be observed for Case 3, in relation to Cases 0 and 4. For ground based gas turbine engines, this issue can be solved by recovering heat from the exhaust gas, but in the case of aircraft turboshafts this solution is not feasible, due to an excessive added weight of a heat recovery installation.

Case 1 reaches a higher entropy level at the power turbine outlet, than Cases 0 and 2, as well as Case 3, compared to Cases 0 and 4, which may be expected to impact on the cycles efficiency.

Another significant result is the decrease in the power turbine inlet pressure (Section 4) for Cases 1 and 3, which, given the unchanged power turbine inlet temperature for all considered cases will trigger a decrease in the engine shaft power, as well as in the efficiency of the two cycles.

The maximum cycle temperatures, reached in Section S, are slightly higher for Cases 3 and 4 where the second stage of the gas generator turbine is required to develop higher work in order to achieve the gas generator balancing. This is a consequence of the fact that, by imposing the reference expansion ratio in the first stage of the gas generator turbine, the work obtained in Cases 3 and 4 is lower than in Cases 1 and 2.

The secondary combustion and turbine expansions processes are presented in Fig. 5 for highlighting the differences observed between the five cases.

TABLE I
REFERENCE THERMODYNAMIC CYCLE

State	p [Pa]	T [K]	h [J/kg]	s [J/kg·K]
0	101,325	288	288,098.35	6,660.12
1	100,312	288	288,098.35	6,663.01
2	722,245	550	554,756.14	6,753.86
3	693,355	1,123	1,187,582.00	7,548.75
4´	454,917	1,030	1,080,382.89	7,570.25
4	222,490	888	919,584.22	7,607.96
5	102,348	752	769,232.16	7,647.22
6	101,325	750	767,088.65	7,647.25

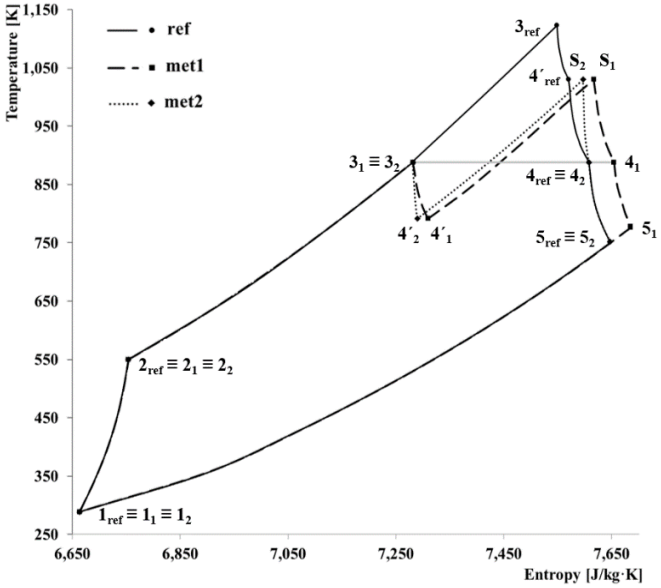

Fig. 3 The thermodynamic cycles for cases 1 and 2, compared to the reference cycle

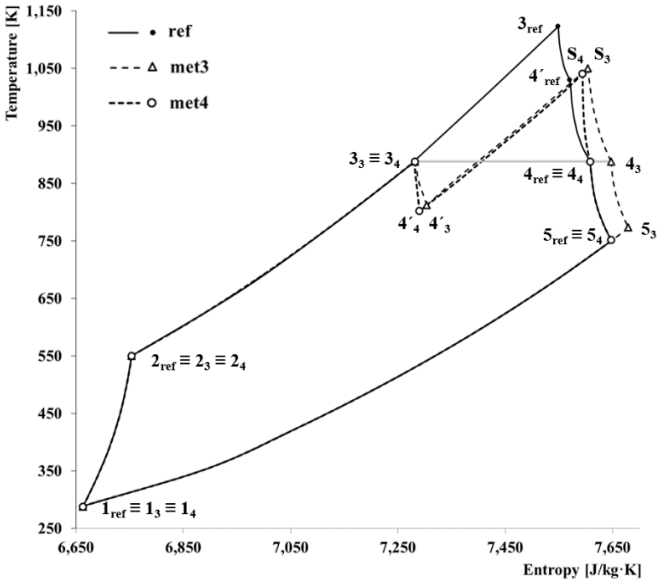

Fig. 4 The thermodynamic cycles for cases 3 and 4, compared to the reference cycle

TABLE II
COMBUSTOR TURBINE THERMODYNAMIC CYCLE 1

State	p [Pa]	T [K]	h [J/kg]	s [J/kg·K]
0	101,325	288	288,098.35	6,660.12
1	100,312	288	288,098.35	6,663.01
2	722,245	550	554,756.14	6,753.86
3	693,355	888	919,588.28	7,281.40
4´	402,909	791	812,389.17	7,309.57
S	386,793	1,030	1,080,386.94	7,616.86
4	189,173	888	919,588.28	7,654.57
5	102,348	778	798,150.30	7,685.06
6	101,325	776	795,931.19	7,685.10

TABLE III
COMBUSTOR TURBINE THERMODYNAMIC CYCLE 2

State	p [Pa]	T [K]	h [J/kg]	s [J/kg·K]
0	101,325	288	288,098.35	6,660.12
1	100,312	288	288,098.35	6,663.01
2	722,245	550	554,756.14	6,753.86
3	693,355	888	919,588.28	7,281.40
4´	431,818	791	812,389.17	7,289.63
S	414,545	1,030	1,080,382.89	7,596.95
4	222,490	888	919,584.22	7,607.96
5	102,348	752	769,232.37	7,647.22
6	101,325	750	767,089.06	7,647.25

TABLE IV
COMBUSTOR TURBINE THERMODYNAMIC CYCLE 3

State	p [Pa]	T [K]	h [J/kg]	s [J/kg·K]
0	101,325	288	288,098.35	6,660.12
1	100,312	288	288,098.35	6,663.01
2	722,245	550	554,756.14	6,753.86
3	693,355	888	919,588.28	7,281.40
4´	454,917	812	835,051.41	7,302.95
S	436,720	1,050	1,103,049.19	7,603.76
4	194,301	888	919,588.28	7,646.89
5	102,348	774	793,296.94	7,678.81
6	101,325	772	791,090.24	7,678.84

TABLE V
COMBUSTOR TURBINE THERMODYNAMIC CYCLE 4

State	p [Pa]	T [K]	h [J/kg]	s [J/kg·K]
0	101,325	288	288,098.35	6,660.12
1	100,312	288	288,098.35	6,663.01
2	722,245	550	554,756.14	6,753.86
3	693,355	888	919,588.28	7,281.40
4´	454,917	803	824,611.26	7,290.01
S	436,720	1,041	1,092,604.97	7,593.77
4	222,490	888	919,584.22	7,607.96
5	102,348	752	769,232.37	7,647.22
6	101,325	750	767,089.06	7,647.25

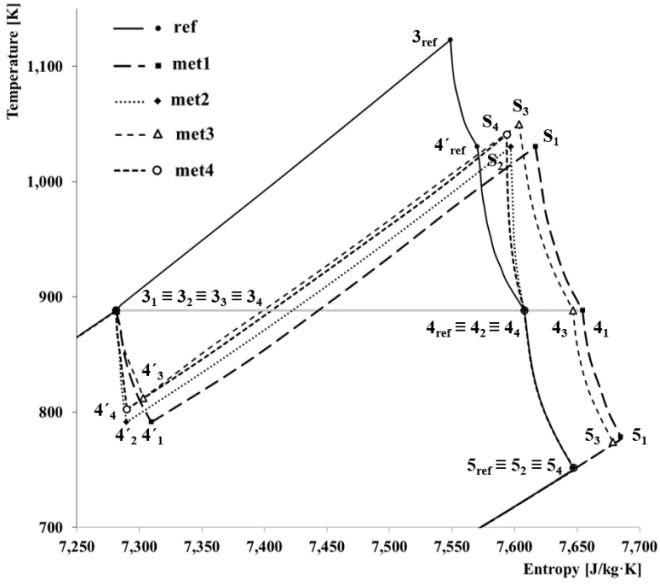

Fig. 5 Detail of the thermodynamic processes representation of the five cycles (Section 3 – Section 5)

TABLE VI
PERFORMANCES OF THE FIVE CYCLES

Cycle	P [kW]	Q_{CC} [J/kgK]	Q_{SC} [J/kgK]	η [%]
0	1,100	632,826.86	0	23.046
1	888	365,832.14	267,997.77	18.614
2	1,100	365,832.14	267,997.77	23.046
3	924	365,832.14	267,997.77	19.358
4	1,100	365,832.14	267,997.77	23.046

For a clearer view of the effect of the turbine combustion on the engine thermodynamic performances, the engine shaft power and thermodynamic efficiency are determined based on the above presented results, according to expressions [48]:

$$P_{PT} = w_{PT} \cdot \dot{M}_a, \tag{59}$$

The thermal efficiency of the reference cycle is

$$\eta_{th} = \frac{P_{PT}}{\frac{Q_{CC}}{\eta_{CC}} \cdot \dot{M}_a}. \tag{60}$$

while the thermal efficiency of the other four cycles is given by:

$$\eta_{th} = \frac{P_{PT}}{\left(\frac{Q_{CC}}{\eta_{CC}} + \frac{Q_{SC}}{\eta_{SC}}\right) \cdot \dot{M}_a}. \tag{61}$$

It can be seen that both the shaft power and the cycle efficiency decrease in Cases 1 and 3, as compared to the reference case, mainly due to the observed decrease in the power turbine inlet pressure, but also related to the observed increase in entropy at the power turbine outlet, which causes an increase in enthalpy on the same isobar. Approximately the same percentage is observed for the decrease in power as well as in cycle efficiency for each of the two cases, of 19% in Case 1 and 16% in Case 3.

However, if Case 2 and Case 4, where the efficiencies of the gas generator turbine stages are increased such that the entropy at the power turbine outlet is maintained at the same value as in the reference Case 0, the engine shaft power is kept constant, also maintaining the cycle efficiency. In order to achieve this, the Case 2 turbine stages efficiencies had to be raised to 0.943, while the Case 4 turbines required a slightly lower efficiency of 0.933.

The heat introduced by combustion in the main combustor decreases, as expected, for the turbine combustor cases, by 42%, and the remaining heat is, instead, introduced in the turbine combustor.

IV. CONCLUSION

The results indicate that maintaining the same temperature at the power turbine inlet and the same power/expansion ratio distribution between the two gas generator turbine stages actually worsen the thermodynamic performances in a

theoretical combustion turbine cycle. In other words, the reduction in the maximum cycle temperature, and, consequently, of the NO_x emissions, comes at the cost of reducing both the power and the efficiency of a gas turbine engine.

A solution to alleviate this is, as shown by Cases 2 and 4, to increase the efficiency of the gas generator turbine stages, which, if sufficiently large may produce the same amount of shaft power while maintaining an initial cycle efficiency.

Further studies are planned to extend research to multiple stage turbines and to multiple fuel injectors per stage in an effort to closer approximate the behaviour of an isothermal expansion turbine.

ACKNOWLEDGMENT

The research work presented herein was funded by the Romanian National Research Program "Partnerships in priority fields", research project "Gas Turbine using *in situ* combustion – TURIST", contract no. 286/2014.

REFERENCES

[1] R.T. Balmer, "Modern Engineering Thermodynamics", Academic Press, 2011

[2] W. A. Sirignano, D. Dunn-Rankin, F. Liu, B. Colcord, S. Puranam, "Turbine Burners: Flameholding in Accelerating Flow", AIAA 2009 - 5410 in *Proc. 45th AIAA/ASME/SAE/ASEE Joint Propulsion Conf. and Exhibit*, Denver, Colorado, USA, August 2009

[3] D. G. Elliot, "Two-Fluid Magneto-Hydrodynamic Cycle for Nuclear-Electric Power Generation", *ARS J*., vol. 32, pp. 924-924, 1963

[4] F. Liu, W.A. Sirignano, "Turbojet and Turbofan Engine Performance Increases through Turbine Burners", *J. Prop. Power*, vol. 17, pp. 698-705, 2001

[5] F. E. Marble, T. C. Adamson Jr., "Ignition and Combustion in a Laminar Mixing Zone", *Jet Prop*., vol. 24, pp. 85, 1954

[6] H. W. Emmons, "Thin Film Combustion of Liquid Fuel", *Zeitschrift für Angewandte Mathematik und Mechanik*, vol. 36, pp. 60, 1956

[7] P. M. Chang, "Chemically Reacting Nonequilibrium Boundary Layers", in "*Advances in Heat Transfer*", J.P. Hartnett and T.F. Irvine Jr., Ed., New York: Academic Press , 1965, pp. 109 - 270

[8] O. P. Sharma, W. A. Sirignano, "On the Ignition of a Premixed Fuel by a Hot Projectile", *Comb. Sci. Tech.*, vol 1, pp. 481-494, 1970

[9] S. V. Patankar, D.B. Spalding, *Heat and Mass Transfer in Boundary Layers*, London: Intertext, UK, 1970

[10] P. Givi, J. I. Ramos, W. A. Sirignano, "Probability Density Function Calculation in Turbulent Chemically Reacting Round Jets, Mixing Layers and One-dimensional Reactors", *J. Non-Equilibrium Thermodynamics*, vol. 10, pp. 75-104, 1985

[11] J. Buckmaster, T. L. Jackson, A. Kumar, *Combustion in High-Speed Flows*, Dordrecht Kluwer Academic, 1994

[12] C. E. Grosch, T.L. Jackson, "Ignition and Structure of a Laminar Diffusion Flame in a Compressible Mixing Layer with Finite Rate Chemistry", *Phys. Fluids A*, vol. 3, pp. 3087-3097, 1991

[13] T. L. Jackson, M. Y. Hussaini, "An Asymptotic Analysis of Supersonic Reacting Mixing Layers", *Comb. Sci. Tech.*, vol. 57, pp. 129, 1988

[14] H. G. Im, B. H. Chao, J. K. Bechtold, C.K. Law, "Analysis of Thermal Ignition in the Supersonic Mixing Layer", *AIAA J.*, vol. 32, pp. 341-349, 1994

[15] H. G. Im, B. T. Helenbrook, S. R. Lee, C. K. Law, "Ignition in the Supersonic Hydrogen / Air Mixing Layer with Reduced Reaction Mechanisms", *J. Fluid Mech.*, vol. 322, pp. 275-296, 1996

[16] D. Chakraborty, H.V.N. Upadhyaya, P.J. Paul, H.S. Mukunda, "A Thermo-chemical Exploration of a Two-dimensional Reacting Supersonic Mixing Layer", *Phys. Fluids*, vol. 9, no. 11, pp. 3513-3522, 1997

[17] W.A. Sirignano, I. Kim, "Diffusion Flame in a Two-dimensional Accelerating Mixing Layer", *Phys. Fluids*, vol. 9, no. 9, pp. 2617-2630, 1997

[18] X. Fang, F. Liu, W.A. Sirignano, "Ignition and Flame Studies for an Accelerating Transonic Mixing Layer", *J. Prop. Power,* vol. 17, no. 5, pp. 1058-1066, 2001

[19] C. Mehring, F. Liu, W.A. Sirignano, "Ignition and Flame Studies for a Turbulent Acceleration Transonic Mixing Layer" in *Proc. 39th Aerospace Sciences Meeting*, AIAA-2001-1096, Reno, Nevada, USA, January 2001

[20] J. Cai, O. Icoz, F. Liu, W.A. Sirignano, "Ignition and Flame Studies for Turbulent Transonic Mixing in a Curved Duct Flow" in *Proc. 39th Aerospace Sciences Meeting*, AIAA-2001-0189, Reno, Nevada, USA, January 2001

[21] J. Cai, O. Icoz, F. Liu, W.A. Sirignano, "Combustion in a Transonic Turbulent Flow with Large Axial and Transverse Pressure Gradients" in *Proc. 18th ICDERS*, Seattle, Washington, USA, July - August 2001

[22] F. Cheng, F. Liu, W.A. Sirignano, "Nonpremixed Combustion in an Accelerating Turning, Transonic Flow Undergoing Transition", *AIAA J.*, vol. 45, pp. 2935-2946, 2007

[23] F. Cheng, F. Liu, W.A. Sirignano, "Nonpremixed Combustion in an Accelerating Transonic Flow Undergoing Transition", *AIAA J*, vol. 46, pp. 1204-1215, 2008

[24] F. Cheng, F. Liu, W.A. Sirignano, "Reacting Mixing-Layer Computations in a Simulated Turbine Stator Passage", *J. Prop. Power*, vol. 25, no. 2, 2009

[25] J. Zelina, G.J. Sturgess, D.T. Shouse, "The Behaviour of an Ultra-Compact Combustor (UCC) Based on Centrifugally - Enhanced Turbulent Burning Rates", in *Proc. 40th AIAA/ASME/SAE/ASEE Joint Propulsion Conf. and Exhibit*, Fort Lauderdale, FloridAIAA-2004-3541, July 2004

[26] R.J. Quaale, R.A. Anthenien, J. Zelina, J. Ehret, "Flow Measurements in a High Swirl Ultra Compact Combustor for Gas Turbine Engines", in *Proc. 16th ISABE Conf.*, ISBAE 2003-1141, Cleveland, Ohio, USA, September 2003

[27] J. Zelina, D.T. Shouse, R.D. Hancock, "Ultra-Compact Combustors for Advenced Gas Turbine Engines", in *Proc. ASME Turbo Expo 2004*, 2004-GT-53155, Vienna, Austria, June 2004

[28] J. Zelina, G.J. Sturgess, A. Mansour, R.D. Hancock, "Fuel Injection Design Optimization for an Ultra-Compact Combustor", in *Proc. 16th ISABE Conf.*, ISABE 2003-1079, Cleveland, Ohio, USA, September 2003

[29] K.C. Lin, K.A. Kirdendall, P.J. Kennedy, T.A. Jackson, "Spray Structures of Aerated Liquid Fuel Jets in Supersonic Crossflows", in *Proc. 35th AIAA/ASME/SAE/ASEE Joint Propulsion Conf.,* AIAA-99-2374, Los Angeles, California, USA, June 1999

[30] K.C. Lin, P.J. Kennedy, T.A. Jackson, "Spray Penetration Heights of Angle Injected Aerated Liquid Jets in Supersonic Crossflows", in *Proc. 38th Aerospace Sciences Meeting,* AIAA-2000-0194, Reno, Nevada, USA, 2000

[31] K.Y. Hsu, C. Carter, J. Crafton, M. Gruber, J. Donbar, T. Mathur, D. Schommer, W. Terry, "Fuel Distribution About a Cavity Flameholder in Supersonic Flow", in *Proc. 36th AIAA/ASME/SAE/ASEE Joint Propulsion Conf.,* AIAA-2000-3585, Huntsville, Alabama, USA, July 2000

[32] T. Mathur, S. Cox-Staufer, K.Y. Hsu, J. Crafton, J. Donbar, M. Gruber, "Experimental Assessment of a Fuel Injector for Scramjet Applications", in *Proc. 36th AIAA/ASME/SAE/ASEE Joint Propulsion Conf.,* AIAA-2000-3703, Huntsville, Alabama, USA, July 2000

[33] M. Gruber, J. Donbar, T. Jackson, T. Mathur, D. Eklund, F. Bilig, "Performance of an Aerodynamic Ramp Fuel Injector in a Scramjet Combustor", in *Proc. 36th AIAA/ASME/SAE/ASEE Joint Propulsion Conf.,* AIAA-2000-3708, Huntsville, Alabama, USA, July 2000

[34] T. Mathur, K.C. Lin, P.J. Kennedy, M. Gruber, J. Donbar, T. Jackson, F. Bilig, "Liquid JP-7 Combustion in a Scramjet Combustor", in *Proc. 36th AIAA/ASME/SAE/ASEE Joint Propulsion Conf.,* AIAA-2000-3581, Huntsville, Alabama, USA, July 2000

[35] G. Yu, J.G. Li, X.Y. Chang, L.H. Chen, "Investigation of Fuel Injection and Flame Stabilization in Liquid Hydrocarbon - Fueled Supersonic Combustion", in *Proc. 36th AIAA/ASME/SAE/ASEE Joint Propulsion Conf.*, AIAA-2000-3581, Huntsville, Alabama, USA, July 2000

[36] G. Yu, J.G. Li, X.Y. Chang, L.H. Chen, C.J. Sung, "Investigation on Combustion Characteristics of Kerosene Hydrogen Dual Fuel in a Supersonic Combustor", in *Proc.36th Joint Propulsion Specialists Meeting,* AIAA-2000-3620, 2000

[37] W.A. Sirignano, D. Dunn-Rankin, F. Liu, B. Colcord, S. Puranam, "Turbine Burners: Flameholding in Accelerating Flow", in *Proc. 45th*

AIAA/ASME/SAE/ASEE Joint Propulsion Conf. and Exhibit, AIAA 2009 - 5410, Denver, Colorado, USA, August 2009

[38] D.T. Shouse, R.C. Hendricks, D.L. Burrus, W.M. Roquemore, R.C. Ryder, B.S. Duncan, N.S. Liu, A. Brankovic, J.A. Hendricks, J.R. Gallagher, "Experimental and Computational Study of Trapped Vortex Combustor Sector Rig with Tri-pass Diffuser". *NASA Report*, Glenn Research Center, 2004

[39] A. Lapsa, J.A. Dahm, "Experimental Study on the Effects of Large Centrifugal Forces on Step Stabilized Flames", in *Proc. 5th US Combustion Meeting*, San Diego, California, USA, March 2007

[40] J. Zelina, D.T. Shouse, G.J. Sturgess, W.M. Roquemore, "Emissions Reduction Technologies for Military Gas Turbine Engines", *J. Prop. Power*, vol. 21, no. 2, 2004

[41] R.S. Bunker, "Integration of New Aero-thermal and Combustion Technologies with Long Term Design Philosophies for Gas Turbine Engine", in *Proc. US Ukrainian Workshop on Innovative Combustion and Aerothermal Technologies in Energy and Power Systems*, Kiev, Ukraine, May 2001

[42] C. Stone, S. Menon, "Simulation of Fuel / Air Mixing and Combustion in a Trapped Vortex Combustor", in *Proc. 38th AIAA Aerospace Sciences Meeting and Exhibit*, AIAA-2000-0478, Reno, Nevada, USA, 2000

[43] J. Zelina, "Numerical Studies on Cavity Inside Cavity Supported in Ultra Compact Combustors", in *Proc. ASME Turbo 2008*, Berlin, Germany, June 2008

[44] D.T. Shouse, J. Zelina, R.D. Hancock, "Operability and Efficiency Performance of Ultra-compact, High Gravity (g) Combustor Concepts", in *Proc. ASME Turbo 2006*, Barcelona, Spain, May 2006

[45] T.E. Lippert, R.A. Newby, D.M. Bachovchin, "Gas Turbine Reheat using In-situ Combustion", *Topical Report: Task 4. Conceptual Design and Development Plan.,* 2004

[46] T.E. Lippert, R.A. Newby, D.M. Bachovchin, "Gas Turbine Reheat using In-situ Combustion", *Topical Report: Task 4. Conceptual Design and Development Plan.,* 2004

[47] European Commission, *Flightpath 2050 Europe's Vision for Aviation*, Luxembourg: Publications Office of the European Union, 2011

[48] V. Pimnsner - "Motoare aeroreactoare. Vol. I" Editura Didactica si Pedagogica, Bucuresti, 1983

[49] Klimov Corporation, "Motorul de aviatie turbopropulsor TV2-117A si reductorul VR-8", Ministerul Transporturilor si Telecomunicatiilor, Bucuresti, 1973

[50] V. Stanciu - "Motoare aeroreactoare (Indrumar de anteproiectare)". Institutul Politehnic Bucuresti. Facultatea de Aeronave. Bucuresti, Romania, 1992